Journal of Applied Mechanics and Technical Physics, Vol. 36, No. 6, 1995

HYPERSONIC FLOW ON A FLAT PLATE. EXPERIMENTAL RESULTS AND NUMERICAL MODELING

V. N. Vetlutskii, A. A. Maslov, S. G. Mironov, T. V. Poplavskaya, and A. N. Shiplyuk

UDC 532.526

The study of hypersonic flow about different types of bodies has assumed increasing importance with the progress that has been made in the design of spacecraft. Existing hypersonic wind tunnels do not permit complete modeling of flight conditions at high Mach numbers ($M_\infty \geq 20$). In addition, only certain gasdynamic parameters can be measured in experiments. This has enhanced the importance of methods for numerically modeling hypersonic flows. Such modeling makes it possible to simultaneously determine all of the parameters of a flow within the framework of the chosen model throughout the investigated region. However, no modeling is absolute, and the results must be substantiated by comparison with experimental data. On the other hand, combining these two approaches also gives the researcher greater confidence that the experimental methodology is correct.

A common object of investigation is the flow on a plate with a sharp edge at a zero angle of attack. The electron-beam [1-4] and electron-probe [5] methods were used earlier to measure the distribution of mean density near the sharp edge of a plate for low Reynolds numbers ($Re_x < 3 \cdot 10^4$). There is no measurement data for higher Reynolds numbers. Results of a numerical study of hypersonic flow past a plate in a locally self-similar approximation were presented in [6]. This problem was solved more accurately in [7], where allowance was made for the structure of the shock wave (SW). The region of applicability of the Rankine–Hugoniot conditions on the wave were determined. Both investigations studied the region near the leading edge of the plate, where the local Reynolds numbers were on the order of 10^4.

In this study, we describe the experiment and present results of use of the method of electron-beam fluorescence to measure profiles of density in the flow of nitrogen about a plate at a zero angle of attack. The experiments were conducted with a Mach number for the incoming flow $M_\infty = 21$ and a unit Reynolds number per meter $Re_1 = 6 \cdot 10^5$. The model of a viscous shock layer was used to develop an algorithm to calculate hypersonic flow about the plate. We present calculated profiles of velocity, temperature, and density. The latter are compared with the experiment in a number of the sections.

1. Experimental Method. The measurements were made in hypersonic nitrogen wind tunnel T-327 at the ITPM (Institute of Theoretical and Applied Mechanics of the Siberian branch of the Russian Academy of Sciences) [8] with stagnation parameters $P_0 = 8$ MPa, $T_0 = 1100$ K. The radius of the uniform core of the flow was $5 \cdot 10^{-2}$ m, while the density of the particles in the flow was $7 \cdot 10^{21}$ m^{-3}. The density of the flow decreased rapidly outside the core, reaching $\approx 6 \cdot 10^{20}$ m^{-3} at a distance of 0.1 m from the axis.

The plate model was in the form of a trapezoid. The widths of the leading and trailing edges were $8 \cdot 10^{-2}$ and $6 \cdot 10^{-2}$ m and the length of the plate $L = 3.6 \cdot 10^{-1}$ m. The leading edge of the plate had the form of a wedge with an angle of 7°. The radius of curvature of the leading edge was less than $5 \cdot 10^{-5}$ m, which was comparable to the mean free path of the molecules in the incoming flow. The plate was made of blackened aluminum. During the experiment, plate temperature changed within the range 290-320 K due to the heating of the flow.

The density of the gas in the flow was determined from the intensity of fluorescence of nitrogen under the influence of electrons in the diagnostic beam [9]. The energy of the electrons was 10-12 keV, beam current did not exceed 1 mA, and the diameter of the beam under the high-vacuum conditions was 10^{-3} m. The beam travelled across the flow parallel to the plane of the plate. The measurement point along a normal to the plate was scanned by moving the plate within the range $-2 \cdot 10^{-2} \ldots +3 \cdot 10^{-2}$ m relative to the axis of the flow. Scanning along the plate was done by deflecting the beam with a magnetic system and moving the electron gun.

Institute of Theoretical and Applied Mechanics, Siberian Branch of the Russian Academy of Sciences, 630090 Novosibirsk. Translated from Prikladnaya Mekhanika i Tekhnicheskaya Fizika, Vol. 36, No. 6, pp. 60-67, November-December, 1995. Original article submitted December 16, 1994.

 0021-8944/95/3606-0848$12.50

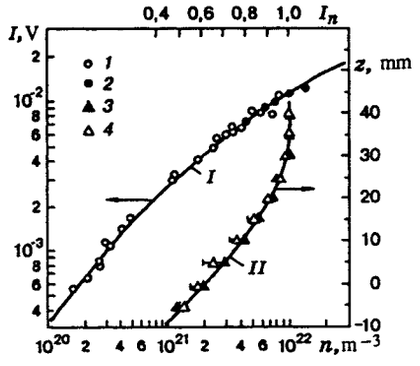

Fig. 1

Nitrogen fluorescence was recorded by photoelectric multiplier FEU-79. The optical system included a rapid objective, a broadband glass filter SS-8 (λ = 350-520 nm), and a diaphragm limiting the field of view of the photomultiplier (PMP) to $1.7 \cdot 10^{-3}$ m across the beam and 10^{-2} m along the beam. The direction of the axis of observation coincided with a normal to the surface passing through the plane of symmetry of the plate. The use of an SPM-2 spectrometer to measure the composition of the radiation reaching the PMP showed that the spectrum corresponds to radiation of the first negative and second positive band, with the ratio of the total intensities equal to 7:1.

A calibration curve was constructed to determine values of density from the signal of the PMP. Figure 1 shows data from measurements of signal I in the stationary gas and in the free hypersonic flow (points 1 and 2). The values of density n in the stationary gas were measured with a McLeod gage, while density in the flow was calculated using isentropic relations. The satisfactory agreement between the data indicates that the broadband radiation is only slightly dependent on the static temperature of the gas. The measurement results were extrapolated by means of generalizing curve I (Fig. 1) to the high-density region, corresponding to values that existed behind the shock wave and were inaccessible during calibration of the system. They have the analytic expression

$$I = bn\Phi\left(\frac{a}{\sqrt{n}}\right), \tag{1.1}$$

where $a = 4 \cdot 10^{10}$ m$^{-3/2}$; b = $6.7 \cdot 10^{-24}$ V·m^{-3}; Φ is the error integral; n is density. Expression (1) was obtained in accordance with the model in [10], which considers only the scattering of primary beam electrons with a radial Poisson distribution on the gas molecules. The deviation of the experimental points from the generalizing curve lies within the range $\pm 6\%$. Such a calibration curve can be used to determine density in two cases: for sufficiently low densities, where the dependence is linear; when the scales of the measured and calibrated gas volumes are equal along the electron beam. Here, density within the scale should be constant. The second case corresponds to flow past two-dimensional bodies (plate, wedge, etc.) whose transverse dimensions are comparable to or greater than the core of the incoming flow. The direction of the axis of the electron beam should be parallel to the plane of the bodies. Our experiment met these conditions.

The principle of calibration employed and the use of the given model [10] were substantiated by measurements of attenuation of the PMP signal during scanning of the point of observation along the axis of the beam. Figure 1 shows dimensionless values of the PMP signal I_n in relation to the distance z from the plane of symmetry of the plate (point 3 corresponds to the free flow, point 4 corresponds to the flow in the region behind the SW). The horizontal intervals show the scatter of the measurements in different sections of the plate. In order to be able to compare different sets of data, the distributions along z were normalized with respect to their maxima ($I_* = I(z)/I_{max}$) and referred to the same scale by means of the relation

$$I_n = 1 + \frac{I_*(z) - 1}{2I_*(-5)}.$$

Curve II in Fig. 1 shows the relation in the form $\Phi(c/(40 - z)^{3/2})$, which follows from the model [10] (c is a constant). The good agreement between the different measurements and between the measurements and curve II substantiates the assumptions made in our approach. The data in [9, 11] also shows that, for the conditions of our experiment, the intensities of the processes

of extinction by collision and absorption of radiation were considerably lower than the process of scatter of primary electrons. Nitrogen luminescence excited by secondary electrons is considered in calibration but may affect measurement accuracy in regions in which there is a rapid change in density in the direction of the optical axis due to the finite depth of focus of the objective. In particular, scattering of the primary beam and secondary luminescence "blur" the front of the shock wave and shift the maximum of density toward the surface of the plate. The true position of the wave can be determined by reconstructing the distribution of density through the solution of a convolution-type integral equation with a Fourier transform.

The kernel of the equation is the instrument function, which includes the broadening of the primary beam, secondary luminescence of nitrogen, and the final width of the diaphragm of the optical system. Its specific form can be obtained from the dependence of the decay of the PMP signal at the projection of the observation point in the undistrubed flow. For most measurements, the function is described well by the relation $\exp(-|y|/(1.8\cdot10^{-3}))$, where y is a coordinate, m. The experimental data was smoothed by polynomials in reconstructing the flow. Determining the function made it possible to refine the position of the SW, but this resulted in a distortion of the density distribution in the direction of the plate surface. As was shown by measurements of the luminescence profile, this distortion was connected with significant contraction of the scale of luminescence of the gas in the lower-density regions between the plate and the point of the density maximum.

Thus, the instrument function is not universal but instead depends on the measurement point. This complicates the problem of reconstructing the flow considerably. On the other hand, the narrowness of the function makes it possible to reliably measure density between the plate and the region adjacent to the SW. We did not observe that the conductivity of the plate had an effect on luminescence intensity in the stationary gas up to the moment it came into contact with the beam of primary electrons. This small region can be excluded from the measurements.

2. Numerical Study. At large Mach numbers and small Reynolds numbers, the thickness of the boundary layer is commensurate with the distance over which decay of the shock wave takes place. Thus, the model of a viscous shock layer is a good approximation for such flows. By a viscous shock layer, we mean the region between the SW and the surface of the body within which the effects of viscosity and heat conduction are significant. In the present study, we are examining hypersonic flow past a flat plate with a sharp leading edge at a zero angle of attack. The flow is studied within the framework of the two-dimensional equations of a complete viscous shock layer (CVSL). These equations can be obtained in a manner similar to [12] and appear as follows in a cartesian coordinate system (x, y)

$$
\begin{aligned}
&\frac{\partial \rho u}{\partial x}+\frac{\partial \rho v}{\partial y}=0,\\
&\rho u\frac{\partial u}{\partial x}+\rho v\frac{\partial u}{\partial y}-\frac{1}{\mathrm{Re}_L}\frac{\partial}{\partial y}\left(\mu\frac{\partial u}{\partial y}\right)+\frac{\partial P}{\partial x}=0,\\
&\rho u\frac{\partial v}{\partial x}+\rho v\frac{\partial v}{\partial y}-\frac{4}{3}\frac{1}{\mathrm{Re}_L}\frac{\partial}{\partial y}\left(\mu\frac{\partial v}{\partial y}\right)+\frac{\partial P}{\partial y}=0,\\
&c_p\rho u\frac{\partial T}{\partial x}+c_p\rho v\frac{\partial T}{\partial y}-\frac{1}{\mathrm{Pr}}\frac{1}{\mathrm{Re}_L}\frac{\partial}{\partial y}\left(k\frac{\partial T}{\partial y}\right)-\\
&\qquad-\frac{1}{\mathrm{Re}_L}(\gamma-1)\mathrm{M}_\infty^2\mu\left(\frac{\partial u}{\partial y}\right)^2-(\gamma-1)\mathrm{M}_\infty^2\left(u\frac{\partial P}{\partial x}+v\frac{\partial P}{\partial y}\right)=0,\\
&P=\frac{1}{\gamma\mathrm{M}_\infty^2}\rho T,
\end{aligned}
\qquad (2.1)
$$

where the x axis is directed along the surface of the plate from the leading edge; u and v are components of velocity in the x and y directions; T is temperature; Pr is the Prandtl number; $\mathrm{Re}_L=\rho_\infty U_\infty L/u_\infty$ is the Reynolds number, calculated from the parameters of the incoming flow and the length of the model L. In Eqs. (2.1), density ρ, the projection of velocity, viscosity μ, thermal conductivity k, heat capacity c_p, and temperature are referred to their values in the incoming flow. Pressure P is referred to the doubled velocity head $\rho_\infty U_\infty{}^2$, while the variables x and y are referred to the length of the model L. Dimensionless parameters will be used subsequently in the text and the graphs.

In this study, we are examining a flow region so far removed from the leading edge of the plate that the SW can be replaced by a discontinuity and the boundary conditions behind it are determined by the Rankine–Hugoniot conditions [7]. The latter were taken in generalized form, i.e. with allowance for viscosity and heat conduction behind the SW [13, 14]:

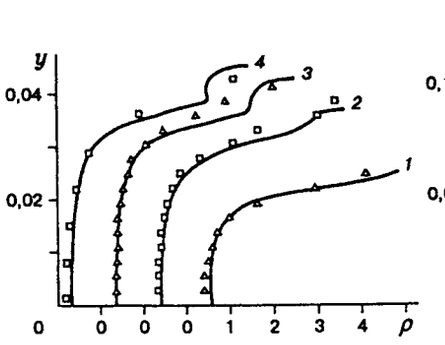

Fig. 2

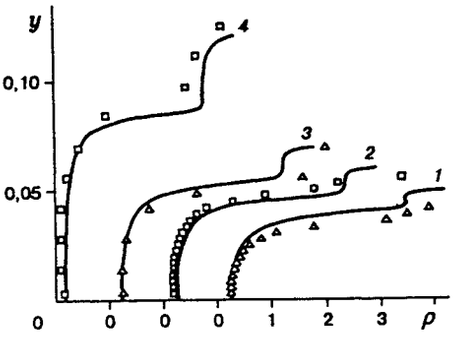

Fig. 3

$$u_s = \cos^2\beta(1 + k_s \operatorname{tg}^2\beta) - \frac{\mu_s(1 - \operatorname{tg}^2\beta)\cos^2\beta}{\mathrm{Re}_L \sin\beta}\frac{\partial u}{\partial y},$$

$$v_s = u_s \operatorname{tg}\beta - k_s \operatorname{tg}\beta, \quad P_s = \frac{1}{\gamma \mathrm{M}_\infty^2} + \sin^2\beta(1 - k_s) - \frac{2\mu_s \sin\beta\cos\beta}{\mathrm{Re}_L}\frac{\partial u}{\partial y},$$

$$H_s = 1 + \frac{\gamma - 1}{2}\mathrm{M}_\infty^2 - \frac{\cos\beta}{\sigma_s \mathrm{Re}_L \sin\beta}\left[\frac{\partial H}{\partial y} - \frac{1 - \mathrm{Pr}}{2}(\gamma - 1)\mathrm{M}_\infty^2 \frac{\partial u^2}{\partial y}\right],$$

$$k_s = \frac{1}{\rho_s}, \qquad \gamma = \frac{c_{p\infty}}{c_{V\infty}}, \qquad \sigma_s = \frac{\mathrm{Pr}}{\mu_s}.$$

Here, H is total enthalpy; β is the angle of inclination of the SW; γ is the adiabatic exponent in the incoming flow. The subscript s corresponds to the parameters of the flow on the inside boundary of the SW.

As the boundary conditions on the plate, we used the conditions of slip and temperature jump [15]:

$$u_w = 1{,}252\frac{2 - \alpha_u}{\alpha_u}\frac{1}{\mathrm{Re}_L}\frac{\mu}{\sqrt{P\rho}}\left.\frac{\partial u}{\partial y}\right|_w,$$
$$T = T_w + 2{,}5\frac{2 - \alpha_T}{\alpha_T}\frac{\gamma}{(\gamma + 1)}\frac{1}{\mathrm{Re}_L}\frac{1}{\mathrm{Pr}}\frac{\mu}{\sqrt{P\rho}}\left.\frac{\partial T}{\partial y}\right|_w. \tag{2.2}$$

In Eqs. (2.2), α_u is the slip coefficient; α_T is the accomodation factor; the subscript w denotes conditions on the wall.

We determined the form of the SW $y_s(x)$ by using an integral condition for the conservation of flow rate with the transition across the SW. We write this condition in dimensionless form as follows

$$\int_0^{y_s(x)} \rho_\infty U_\infty \, dy\Big|_{x=0} = \int_0^{y_s(x)} \rho U \, dy\Big|_x.$$

The angle of inclination of the SW β is determined from the obvious geometric relation $\tan\beta = dy_s/dx$. It should be noted that viscosity was approximated in the calculations by the Sutherland relation.

For convenience in performing the calculations, we introduced a new independent variable in system (2.1) along a normal so that the difference grid had a constant number of cells between the body and the SW (this alleviates the problem of adding points to the grid in the normal direction as the calculations proceed downflow from the initial section). For the same reason, we also introduced new dependent variables by dividing the old variables by their local values behind the SW. Then the equations of momentum and the energy equation were written in the form that is standard for parabolic equations and solved by the routing method together with the continuity equation and equation of state along the coordinate x.

Complete formulation of the problem also requires that we have initial conditions. An analysis of the experimental data in [5, 16] showed that near the sharp edge the viscous flow envelops the entire region between the surface of the plate and the

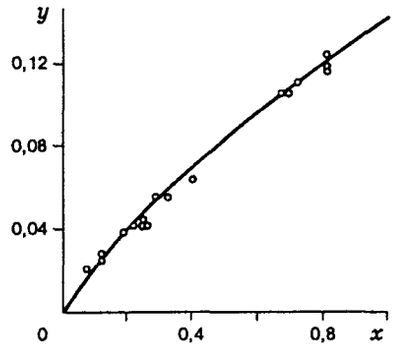

Fig. 4

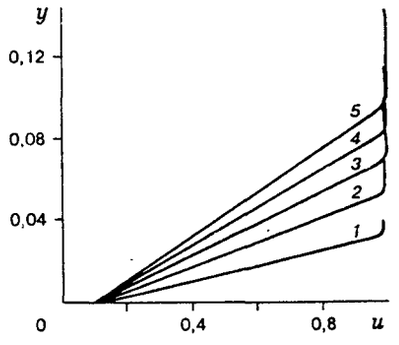

Fig. 5

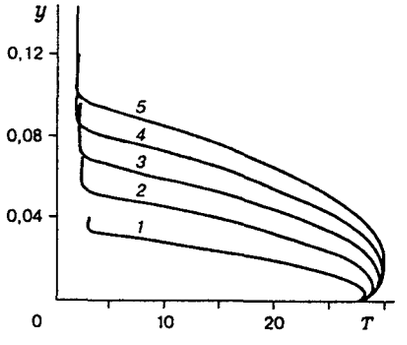

Fig. 6

SW. We thus propose that all of the flow behind the SW near the sharp edge of the plate be described by the equations of the boundary layer. Then system of CVSL equations (2.1) can be reduced to ordinary differential equations by using a transformation of the form $\xi = x$, $\eta = y\sqrt{Re_L}/\sqrt{x}$, which is characteristic of flows in a boundary layer with a uniform externalflow. The solutions of these equations are also taken as initial conditions for the complete equations of the viscous boundary layer. A more detailed formulation of the problem was given in [17].

Since the CVSL equations are analogous to the equations of a compressible boundary layer, we solve them by using an implicit two-layer difference scheme with weights. We used the same scheme previously to solve boundary-layer equations in [18], where the method is described in more detail.

Calculations were performed on a difference grid with the number of points along the normal N = 160. The mesh along the coordinate x was chosen equal to 0.001. The slip coefficient and accomodation factor were taken equal to 0.8 [1].

3. Discussion of Results. The methodology described above was used to perform repeated experiments involving measurement of density in the case of flow past a flat plate with a sharp edge. The resulting data, in the form of the dependence of density on the normal coordinate, is shown by the points in Figs. 2 and 3. Lines 1-4 (the calculated results) in Fig. 2 correspond to the sections x = 0.12, 0.185, 0.22, and 0.235, while the lines in Fig. 3 correspond to the sections x = 0.26, 0.33, 0.4, and 0.81 (triangles are used for the odd-numbered lines, squares for the even-numbered lines).

Calculations of flow past the plate based on the viscous shock layer model were performed with the above experimental conditions. It can be seen from the figures that the agreement between the theoretical and experimental data is satisfactory throughout almost the entire region. The somewhat greater difference near the SW can be explained on the one hand by the fact that the SW was represented as a discontinuity in the model. On the other hand, the error of the experimental values of density increases near the SW due to the scattering of primary electrons and lengthening of the region in which secondary luminescence occurs.

It is evident from Figs. 2 and 3 that the character of the density profiles remains the same over all of the sections. Density changes slightly near the plate surface and then abruptly increases several-fold. Near the SW, the character of the curves changes with an increase in the thickness of the inviscid region.

Figure 4 shows the position of the maximum value of density along the normal (the points show the experimental results, the lines the theoretical results) in relation to the coordinate x. Since the maximum of density is seen immediately after the SW, its position coincides with the position of the wave. The angle of inclination of the wave in the given calculation variant changed from 11° near the leading edge of the plate to 6° on the trailing edge. The agreement between the experimental and theoretical data is satisfactory.

Figures 5 and 6 show profiles of velocity and temperature in the sections x = 0.2, 0.4, 0.6, 0.8, and 1.0 (curves 1-5, respectively). Both functions change appreciably along the normal in the boundary layer and are nearly constant in the inviscid region. It is apparent from the figure that nearly the entire shock layer should be considered viscous in the first section (i.e., near the leading edge of the plate), while a region of inviscid flow appears with increasing distance from the leading edge. Here, the fraction of the shock layer occupied by the boundary layer decreases.

The calculations also showed that pressure along the normal changes by as much as 15%, but only in the inviscid region. This explains the substantial change in density at constant temperature. We should also point out that in the given calculation variant, pressure along the plate (i.e., from the leading to the trailing edge) decreases fivefold.

Thus, we have devised a method of measuring density in hypersonic flow about a flat plate and created an algorithm to calculate flow behind the SW. The agreement obtained between numerical and measured values of density in the flow is a serious argument in support of the correctness of the data and the validity of the chosen flow model and algorithm.

The authors express their deep gratitude to M. I. Muchnii for discussing the findings with us and to B. A. Sapogov and Yu. A. Safronov for assisting in the experiments.

REFERENCES

1. J. C. Lengrand, A. Allegre, A. Chpain, and M. Raffin, "Rarefied flow over a flat plate with a sharp leading edge: DSMC, Navier–Stokes and experimental results," Proc. 8th Int. Symp. on Rarefied Gas Dynamics. Vancouver (1992).
2. S. C. Metcalf, D. C. Lillicrap, and C. J. Berry, "A study of the effect of surface temperature on the shock-layer development over sharp-edged shapes in low-Reynolds-number high-speed flow," in: Rarefied Gas Dynamics, Vol. 1, Ed. L. Trilling and H. Y. Wachman (1969).
3. I. Wada, "Experimental study of low pressure hypersonic flow by using an electron beam densitometer," Rarefied Gas Dynamics, Vol. I, Ed. J. H. Leeuw (1965), pp. 203-214.
4. P. J. Harbour and J. N. Lewis, "Preliminary measurements of the hypersonic rarefied flow on a sharp flat plate using an electron beam probe," Rarefied Gas Dynamics, Vol. 2, 1031-1046 (1967).
5. W. J. McCroskey, S. M. Bogdonoff, and J. G. McDougall, "An experimental model for the sharp flat plate in rarefied hypersonic flow," AIAA J., **4**, No. 9, 98-108 (1966).
6. M. L. Shorenstein and R. F. Probstein, "The hypersonic leading-edge problem," ibid., **6**, No. 10, 91-102 (1968).
7. S. Rudman and S. G. Rubin, "Hypersonic viscous flow over slender bodies with sharp leading edges," ibid., 72-81.
8. G. I. Bagaev, I. G. Druker, V. D. Zhak, et al., "Hypersonic nitrogen wind tunnel T-327A," in: Aerodynamic Investigations [in Russian], Novosibirsk (1972), p. 20.
9. E. P. Muntz, "Measurements of density by analysis of electron beam excited radiation," Methods Exp. Phys., **18**, 434-455 (1981).
10. G. I. Sukhinin, "Spatial distribution of the parameters of the electrons of a diagonostic electron beam," Summary of Documents of the Sixth All-Union Conference on Rarefied Gas Dynamics, Novosibirsk (1979), pp. 79-81.
11. I. E. Beckwith, W. D. Harvey, and E. L. Clark, "Comparison of turbulent boundary layer measurements at Mach number 19.5 with theory and an assessment of probe errors," NASA Report, TN-D-6192. Washington, 1971.
12. R. T. Davis, "Numerical solution of the hypersonic viscous shock-layer equations," AIAA J., **8**, No. 5, 3-13 (1970).
13. I. V. Vershinin, G. A. Tirskii, and S. V. Utyuzhnikov, "Supersonic laminar flow about the windward part of swept wings of infinite dimensions within a broad range of Reynolds numbers," Izv. Akad. Nauk SSSR Mekh. Zhidk. Gaza, No. 4, 40-44 (1991).
14. G. A. Tirskii, "Toward a theory of the hypersonic flow of a viscous chemically reacting gas about flat and axisymmetric bluff bodies in the presence of injection," Nauchn. Tr. In-ta Mekhaniki Mosk. Univ., No. 39, 3-38 (1975).
15. L. G. Loitsyanskii, Mechanics of Liquids and Gases [in Russian], Nauka, Moscow (1973).

16. H. T. Nagamatsu, R. E. Sheer Jr., and J. R. Shchmid, "Flow around the flat plate by the hypersonic flow of dilute gas at high temperatures," ARS J., **31**, No. 7, 58-69 (1961).
17. V. N. Vetlutskii and T. V. Poplavskaya, "Numerical solution of the equations of a viscous shock layer in hypersonic flow past a plate," Computer Technologies: Transactions of a Scientific Conference. Russian Academy of Sciences, Siberian Branch. Institute of Computer Technologies, **4**, No. 12, 61-69 (1995).
18. V. N. Vetlutskii and T. V. Poplavskaya, "Calculation of a laminar boundary layer on flat triangular plate with supersonic leading edges," Chislennye Metody Mekhaniki Sploshnoi Sredy, **13**, No. 1, 31-43 (1982).